



Ex situ measurements of through-plane thermal conductivities in a polymer electrolyte fuel cell

O. Burheim^a, P.J.S. Vie^b, J.G. Pharoah^{a,c,1}, S. Kjelstrup^{a,*}

^a Inst. Kjemi, Realfagsb., 7491 Trondheim, Norway

^b Institute for Energy Technology, 2007 Kjeller, Norway

^c Queen's-RMC Fuel Cell Research Centre, 945 Princess Street, Kingston, ON, Canada K7L 5L9

ARTICLE INFO

Article history:

Received 24 February 2009

Received in revised form 19 June 2009

Accepted 23 June 2009

Available online 2 July 2009

Keywords:

Thermal conductivity

Fuel cell

Nafion

Gas diffusion layer

Water content

ABSTRACT

In this paper thermal properties for materials typically used in the proton exchange membrane fuel cell (PEMFC) are reported. Thermal conductivities of Nafion membranes were measured *ex situ* at 20 °C to be 0.177 ± 0.008 and $0.254 \pm 0.016 \text{ WK}^{-1} \text{ m}^{-1}$ for dry and maximally wetted membranes respectively. This paper also presents a methodology to determine the thermal conductivity of compressible materials as a function of applied load. This technique was used to measure the thermal conductivity of an uncoated SolviCore porous transport layer (PTL) at various compaction pressures. For the dry PTL at 4.6, 9.3 and 13.9 bar compaction pressures, the thermal conductivity was found to be 0.27, 0.36 and $0.40 \text{ WK}^{-1} \text{ m}^{-1}$ respectively and the thermal contact resistivity to the apparatus was determined to be 2.1, 1.8 and $1.1 \times 10^{-4} \text{ m}^2 \text{ KW}^{-1}$, respectively. It was shown that the thermal contact resistance between two PTLs is negligible compared to the apparatus' thermal contact resistivity. For a humidified PTL, the thermal conductivity increases by up to 70% due to a residual liquid saturation of 25%.

© 2009 Elsevier B.V. All rights reserved.

1. Introduction

Good thermal management of the proton exchange fuel cell (PEMFC) is crucial for further development and successful commercialisation of PEMFC technology. Until recently, little attention has been given to the thermal properties of fuel cell materials and components. The single PEMFC consists of the membrane and electrode assembly (MEA) sandwiched between two porous transport layers (PTL), sometimes referred to as gas diffusion layers or backings, which are usually coated with a micro-porous layer (MPL). The catalyst layer, comprised of PTFE, ionomer, carbon and platinum, can be coated either on the MPL, or on the membrane. In PEMFC stacks a series of single cells are separated by bipolar plates. It is a common practice to specify a single operating temperature for a fuel cell, implicitly assuming that fuel cells operate isothermally. In addition, much of the fuel cell modelling literature has also assumed isothermal operation, but even those works that do not, are limited by a lack of availability of thermal property data.

Evidence is now emerging that substantial temperature gradients [1–4] exist in the single PEMFC, and the proper prediction of fuel cell temperature distributions requires good information on the thermal conductivities of all fuel cell components, as well as the possible contact resistances between these components [5].

Vie and Kjelstrup [1,2] reported the first measurements of temperature gradients inside the MEA of a single PEMFC. For a current density of 0.7 A cm^{-2} , the temperature between the catalyst layers and membrane was about 3 °C higher than in the gas channels at the other side of the gas diffusion layer. A similar temperature gradient was observed at both electrodes. At 0.3 A cm^{-2} this difference was about 2 °C. From the measured temperature gradients a combined thermal conductivity of gas diffusion backing and catalyst layer was estimated to $0.19 \pm 0.05 \text{ WK}^{-1} \text{ m}^{-1}$, but inaccuracy in the positioning of the rather large thermocouples imposed a systematic error to this value. Similar elevated temperatures inside the membrane were measured *in situ* by He et al. [4].

Ihonen [6] reported the thermal impedance of a $100 \mu\text{m}$ Sigracet[®] PTL 10-BC PTL. The thermal conductivity was 0.05 and $0.125 \text{ WK}^{-1} \text{ m}^{-1}$ at respectively 1 and 8 bar compaction pressure. No variances in these values were provided.

Recently, Khandelwal and Mench [7] reported the thermal conductivity of nearly dry Nafion[®] for temperatures from 17 to 65 °C at 20 bar compaction pressure. The measurements were based on an approach similar to the one taken in this paper except that the bulk conductivity and sample thickness were assumed to be constant with applied pressure. They reported values in

Abbreviations: MEA, membrane electrode assembly; MPL, micro-porous layer; PEEK, polyether ether ketone; PEMFC, polymer electrolyte membrane fuel cell; PTFE, Teflon (polytetrafluorethylen); PTL, porous transport layer.

* Corresponding author. Tel.: +47 735 94 179; fax: +47 735 50 877.

E-mail addresses: burheim@ntnu.no (O. Burheim), preben.vie@ife.no (P.J.S. Vie), pharoah@me.queens.ca (J.G. Pharoah), signe.kjelstrup@chem.ntnu.no (S. Kjelstrup).

¹ On leave.

Nomenclature

k_i	thermal conductivity ($\text{W K}^{-1} \text{m}^{-1}$)
q_i	heat flux (W m^{-2})
r_i	thermal resistance per unit length ($\text{K W}^{-2} \text{m}^{-1}$)
A_i	area (m^2)
R_i	thermal resistance (K W^{-1})
R''_i	thermal resistivity ($\text{m}^2 \text{K W}^{-1}$)
T_i	temperature (K or $^\circ\text{C}$)
Z_i	thickness (m or μm)

Greek letters

ε	porosity
λ	water per sulphonic group in Nafion

the range $0.10\text{--}0.20 \text{ W K}^{-1} \text{ m}^{-1}$, depending on the temperature. For SIGRACET[®] diffusion media treated with 20 wt.% PTFE they reported a thermal conductivity of $0.22 \pm 0.04 \text{ W m}^{-1} \text{ K}^{-1}$. This value doubled in the absence of PTFE. Toray diffusion media, having a different microstructure and a different binder, was found to have a thermal conductivity of $1.80 \pm 0.27 \text{ W m}^{-1} \text{ K}^{-1}$ at 26°C .

Ramousse et al. [8] reported an efficient thermal conductivity for the gas diffusion layers provided by Quintech and SGL Carbon. Through-plane thermal conductivities were measured to be $0.363 \text{ W K}^{-1} \text{ m}^{-1}$ for the Quintech ($190 \mu\text{m}$), $326 \text{ W K}^{-1} \text{ m}^{-1}$ for the Quintech ($190 \mu\text{m}$), $0.198 \text{ W K}^{-1} \text{ m}^{-1}$ for the Quintech ($190 \mu\text{m}$) and $0.260 \text{ W K}^{-1} \text{ m}^{-1}$ for the SGL Carbon ($420 \mu\text{m}$). By evaluating the grain structure of the carbon fibres in the PTLs Ramousse et al. estimated the parallel-plane thermal conductivity to be from 1.5 up to 3.5 times larger than the through-plane thermal conductivity [8].

There are in principal two classes of methods to measure a thermal conductivity. The first class may be termed transient methods [10], requiring information about the heat capacity of the investigated material. The temperature is recorded with respect to time and position when the surrounding temperature suddenly drops or increases. The laser-flash radiometry technique [11] is an example of a transient method, which may be applied at elevated temperatures. The second class of methods involves a known, controlled

heat flux and measures temperatures at different locations through the sample [12].

The PEMFC materials are difficult to investigate by the transient method due to size and material structure. The heat capacities of PEMFC materials are also scarcely known. Therefore we consider a transient method to impose work beyond what is comprehensive for obtaining thermal conductivities.

In situ measurements of thermal properties in PEMFCs are challenging due to the complexity of the numerous processes taking place during operation. The PTL is a particular challenge, since the bulk properties of the material will change with compression pressure, and the loading in a fuel cell is not homogeneous. More accurate thermal conductivity values of the single components and the thermal contact resistance of the interfaces between the components in the MEA may be determined *ex situ*.

This paper reports, for the first time, measurements of the thermal conductivity of Nafion as a function of water content. It also presents a methodology for determining the change of both the bulk thermal conductivity of a PTL and its contact resistance as a function of applied pressure.

2. Experimental

2.1. Apparatus

In this work a “constant heat flux” method was chosen for the determination of thermal conductivities (k), due to lack of information on heat capacities. An apparatus was designed to give a one-dimensional heat flux (q), by the cylindrical geometry shown in Fig. 1. The sample is positioned at centre of the apparatus and sandwiched between cylinders in a symmetrical manner. The apparatus can accommodate a stack of the sample material, as well as single elements. In order to measure the sample thickness as a function of compaction pressure, two micrometers (Mitutoyo Digimatic Indicator ID-C Series 543) were connected to the upper flange of the apparatus touching down onto the lower flange. From the distance between the upper and lower parts in the presence and absence of a specimen, the actual thickness of the specimen was determined for all compaction pressures. Sample compression was applied using

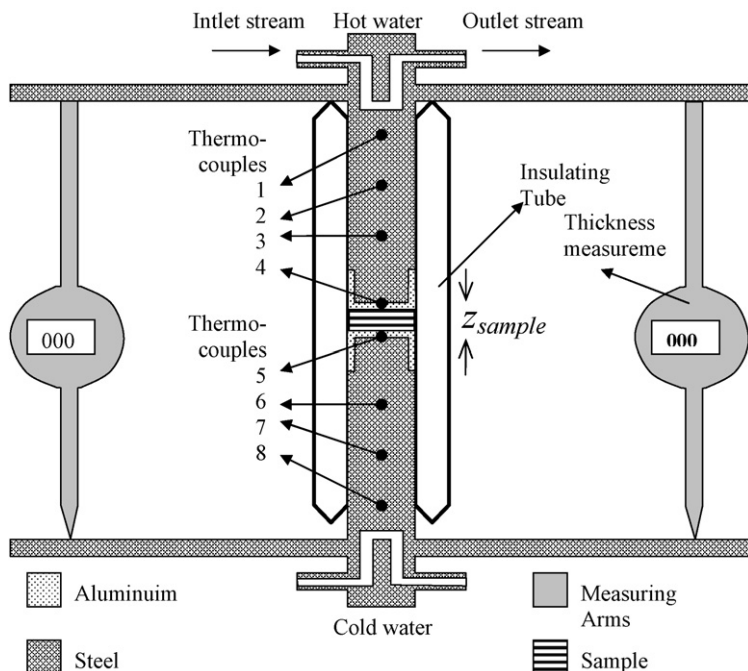


Fig. 1. Sketch of the thermal conductivity apparatus.

a pneumatic piston on one end and a steel ball in the other end to ensure the loading was perpendicular to the sample. The clamping pressure was controlled over a range from 3 to 15 bar; a pressure range consistent with fuel cell conditions.

In order to measure the thermal conductivity, an accurate determination of the one-dimensional heat flux through the device must be made as well as an accurate measurement of the temperature drop across the sample. To this end, the cylinders on each side of the sample were comprised of a large steel section, equipped with three thermocouples (type *k*), capped with a thin aluminium section in contact with the sample. The relatively low value of the thermal conductivity of steel enables good resolution for determining the heat flux while the relatively high thermal conductivity of aluminium provides for an isothermal region adjacent to the sample for determining the temperature drop across the sample. Three thermocouples were used in the steel section to ensure that the temperature profile was linear for the determination of the 1D heat flux. The aluminium disks were screwed onto the ends of the steel rods using a thermal conducting paste in between. Thus the aluminium disk behaves as a large thermometer disk. The diameter of the cylinders and the samples was 21.0 ± 0.1 mm. The heat flux was determined in the upper as well as in the lower part of the apparatus. All eight temperatures were recorded every half minute by an Agilent Acquisition Switch Unit 34970A. In ten minutes the apparatus obtained its stationary state, and the following five minutes were then used for measurements. These thermocouples provide information about temperature differences with a double standard deviation of ± 0.05 K. The two pistons were thus working as heat flux meters giving the heat flux (q), Eq. (2.1), and further the thermal resistance (R) of the sample and its contact thermal resistance towards aluminium, Eq. (2.2). Later, we will use the symbol R'' for the thermal resistivity.

$$q_{upper} = k_{steel} \frac{T_1 - T_3}{l_{1-3}}, \quad q_{lower} = k_{steel} \frac{T_6 - T_8}{l_{6-8}},$$

$$q_{sample} = \frac{q_{upper} + q_{lower}}{2} \quad (2.1)$$

$$R_{total} = R_{sample} + 2R_{Al-sample}; \quad R_{total} = \frac{T_4 - T_5}{q_{sample}},$$

$$R_{sample} = \frac{T_4 - T_5}{q_{sample}} - 2R_{Al-sample} \quad (2.2)$$

$$R_i'' = R_i A_i$$

The overall heat flux was controlled by adjusting the temperatures at each end of the apparatus. This was obtained by circulating hot and cold water through channels in the end pieces, as can be seen in Fig. 1. The temperatures of the heating and cooling water were adjusted to 10 and 35 °C respectively.

In order to obtain a one-dimensional heat flux, the apparatus was thoroughly insulated in the radial direction. The cell was mounted inside a double-walled evacuated glass tube, sealed at both ends. The inside of the double-walls was silver-plated to minimize convection, radiation and thermal conduction in the radial direction.

To assess the temperature profile through the various materials in the thermal conductivity apparatus, a simple mathematical model was used. Room temperature was assumed on the outside surface of the glass tube and thermal conductivity inside the evacuated tube equal to 10% of what it is in air at 1 bar. For the modelling case a 0.5 mm thick PTFE disk was evaluated. The model verified that the aluminium disks were nearly isothermal and that two-dimensional effects at the material interfaces did not interfere with the flux measurement. This indicates that the steel rods provide

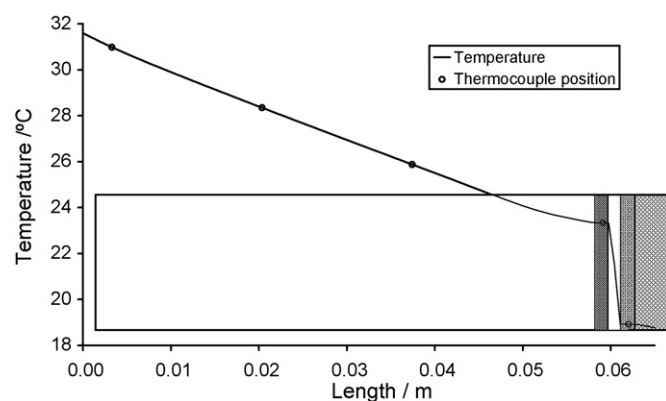


Fig. 2. The modelled temperature profile along with the thermocouple placements for the upper part of the apparatus, including 0.5 mm PTFE sample, also depicting the materials used in Fig. 1.

a suitable temperature gradient between the thermocouples, thus ensuring that heat fluxes may be determined with high accuracy.

The apparatus was calibrated with polytetrafluorethylen, PTFE, following the procedure described below. Disks of PTFE were made with thicknesses ranging from 0.1 to 3.0 mm in order to deconvolute the bulk thermal conductivity from the contact resistance. The thermal conductivity of PTFE was measured to be 0.25 ± 0.10 W K⁻¹ m⁻¹ by both the approaches described below (i.e. Eqs. (2.4) and (2.5)). The thermal conductivity for PTFE is given by a manufacturer [13] to be 0.25 W K⁻¹ m⁻¹. The measured temperature profile along the length of the apparatus was in agreement with Fig. 2.

The thermal contact resistance value between two PTFE disks was found to be between 60% and 70% of the thermal contact resistance value between the apparatus and one PTFE disk (depending on compaction pressure), e.g. $R_{PTFE-PTFE} = 0.6 \times R_{PTFE-Al}$. This result can be explained by two relatively soft surfaces touching each other compared to one hard surface and one soft surface. This also shows that the procedure described below is capable of resolving the bulk thermal conductivity, the thermal contact resistance with the device, and the thermal contact resistance between stacks of samples.

2.2. Procedure

2.2.1. Nafion®

The thermal conductivity of the Nafion® membranes was determined, varying the nominal thickness of the membrane using Nafion® 112 (~51 μm), 115 (~127 μm), 117 (~178 μm) and 1110 (~254 μm), respectively. Each measurement provided the thermal resistance and the actual thickness of the sample, Z_{sample} , at the given clamping pressure. The thickness was, in addition, measured outside the apparatus using a digital micrometer caliper. Eqs. (2.1)–(2.3) explain how we obtained for the sample thermal resistance, R_{sample} , and the thermal conductivity, k_{sample} , based on geometry (area, A , and thickness, Z_{sample}) and thermal resistance respectively. For the lowest and the highest water contents, three disks from each of the four membrane thicknesses were measured. For the intermediate water contents three pieces from two of the membrane thicknesses were used, e.g. three Nafion 112 disks and three Nafion 117 disks.

$$k_{sample} = \frac{Z_{sample}}{R_{sample}A} \quad (2.3)$$

After cutting the membranes into circular disks (Ø21 mm), the disks were cleaned in heated (~80 °C) 1 vol% H₂O₂(aq) (5 min), heated in purified water (10 min), heated in 0.05 M H₂SO₄(aq) (5 min), and finally rinsed in heated purified water (10 min). All

the membrane pieces were then left to dry in an exsiccator for three days, where their water content was found to be 3 ± 1 water molecules per sulphonic group. This was determined by first weighing the samples after being saturated with liquid water ($\lambda = 22 \pm 1$) and then weighing the same samples after vacuum drying them in a glove box where λ was assumed to be 0.5.

According to Zawodzinski et al. [14,15], as well as Pushpa et al. [16], Nafion membranes immersed in pure liquid water will have a water content, λ , of 22 ± 1 water molecules per sulphonic acid group. The desired water level was further obtained by placing three pieces of membrane in a small sealed unit along with the amount of water equal to the expected water uptake, thus using the properties Nafion has as a drying agent. For the driest and most humidified water levels (3 and 22) we used three pieces of all the four thicknesses (twelve measurements per reported value), while we used only two membrane thicknesses for the intermediate water levels (six measurements per reported value).

2.2.2. PTL

The measurement of PTL samples is significantly complicated by the fact that these porous materials deform under load and this deformation results in changes in the bulk thermal conductivity as function of pressure. For this reason it is not possible to deconvolute the contact resistance from the bulk conductivity by simply varying the pressure. Further, PTL materials are not typically available in different thicknesses making the technique used for Nafion difficult to apply. An alternative approach to varying the thickness is to measure samples made up of stacks of different numbers of individual PTLs. This however introduces a new variable, the contact resistance between individual samples, which cannot be isolated with the measured data. Here we present a technique for solving this problem that relies on a hybrid approach, first exploiting the natural sample to sample thickness variation to determine the sample–apparatus contact resistance and then stacks of similar samples to determine the sample to sample contact resistance. This procedure is carried out multiple times at various pressures in order to measure the bulk conductivity as a function of applied load (or alternatively as a function of loaded thickness).

Two kinds of carbon based PTL materials were provided from SolviCore and used in this study. The first kind was a MPL-coated PTL without catalyst (Gas Diffusion Layer Batch-Number # 206-07-1) and the second its uncoated pure carbon paper PTL. The measurement procedure was similar to the one for Nafion® with a few exceptions. Multiple samples were cut ($\varnothing 21$ mm) from a single sheet of PTL material and sorted according to measured thickness, which ranged from 220 to 320 μm . The density of each sample was measured and was found similar in all cases, suggesting that the PTL material is nearly homogeneous in the thickness dimension.

The samples were sorted into three groups, one being very thin (230–250 μm), a second intermediate (270 \pm 5 μm) and a third being fairly thick (300–320 μm). Individual pieces belonging to the thickest and the thinnest groups were evaluated using Eq. (2.4), while stacks of pieces from the intermediate group were evaluated using Eq. (2.5).

In both the experiments the expected measured total thermal resistance, $R_{measured}$, is linear in the thickness. By comparing the y-intercept values from each set of experiments conducted at the same pressure, it is possible to separate the contribution from the thermal contact resistance between two PTL samples.

$$R_{measured} = 2R_{PTL-AI} + r_{PTL}Z_{measured} \quad (2.4)$$

$$R_{measured} = 2R_{PTL-AI} + (n-1)R_{PTL-PTL} + nR_{PTL}$$

$$R_{measured} = (2R_{PTL-AI} - R_{PTL-PTL}) + n(R_{PTL-270} + R_{PTL-PTL}) \quad (2.5)$$

where $R_{PTL-PTL}$ is the contact resistance between two PTLs, R_{PTL-AI} is the thermal contact resistance between the PTL and the apparatus, R_{PTL} is the thermal resistance of PTL alone and r_{PTL} denotes the thermal resistance per unit thickness.

Repeating this procedure at different applied pressures gives the variation of the contact resistance and the bulk conductivity with pressure.

2.2.3. MPL and MEA

The overall thermal resistance for a dry MEA was investigated. In these experiments PTLs coated with MPLs, were used. The Nafion membranes were dry ($\lambda = 3$). The thickness of the MPL was measured by comparing the thickness of the MPL-coated PTL before and after scraping the MPL off the PTL.

2.3. Statistical analysis

The accuracies of the results were evaluated with the classical analysis of variance, ANOVA, Eq. (2.6), and an analysis of the transmissions of errors, Eq. (2.7) [17]. ANOVA gives the standard deviation, s_i , and the confidence interval from the response of selected variables. Measured values, i.e. thermal resistances and thicknesses, results are presented with twice the standard deviation based on Eq. (2.6) or equivalent ANOVA. Eq. (2.7) gives the variance, of any calculated value, e.g. the calculated thermal conductivity.

$$s_i^2 = \frac{\sum_{i=1}^n (y_i - \bar{y})^2}{n-1} \quad (2.6)$$

$$s_i^2 = \sum_{i=1}^p \left(\frac{\partial \lambda}{\partial X_i} s_{X_i} \right)^2 \quad (2.7)$$

3. Results

3.1. Thickness measurements

The accuracy of the measured thermal conductivity is largely determined by the precision of the thickness measurement. This applies to all experiments, and is neglected in previous published works [7,8]. The effect of compression on the PTL is shown in Fig. 3. In this case the compression of the paper is nearly linear with applied load.

Fig. 4 gives the thickness of the MPL-coated PTL, measured with a micrometer calliper outside the apparatus at zero compaction pressure and the established routine for the applied pressures. The figure shows how the thickness of the coated paper varies from 300 μm up to almost 350 μm . The MPL thickness was investigated by measuring the thickness of the MPL-coated PTL before and after

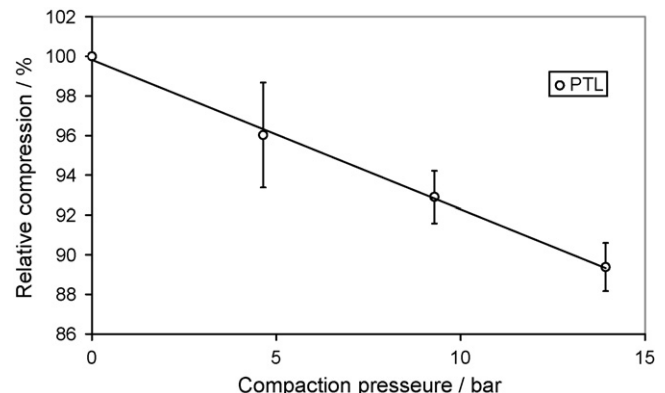


Fig. 3. Relative compression of the PTL as functions of compaction pressure.

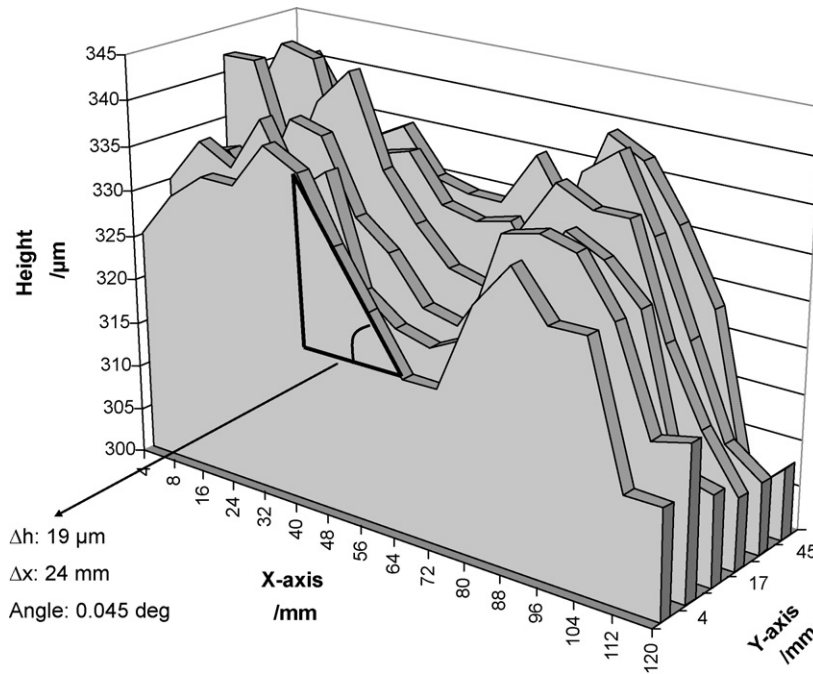


Fig. 4. Measured thicknesses of an MPL-coated PTL at various locations on the paper, obtained by a micrometer calliper.

scraping the MPL off with a surgical blade. The thickness was found to be $71 \pm 21 \mu\text{m}$. There was a weak trend showing that the thinner parts of the PTL had a thicker MPL and vice versa. Thus the MPL-coated PTL had a more uniform thickness than the uncoated PTL.

The manufacturer, DuPont, gives a thickness of Nafion 1110 of $256 \mu\text{m}$, but this value changes considerably with the absorption of water. We measured the average thickness for this membrane as a function of water content, as presented in Table 1.

3.2. The thermal conductivity of Nafion® as a function of water content

We present the measured thermal resistance and the measured thickness, respectively, of Nafion® membranes, from which the thermal conductivities are calculated, before we proceed to report the thermal conductivity as a function of water content in the membrane and of applied compaction pressure.

Fig. 5 presents the measured thermal resistance of a Nafion® membrane and its contact to the apparatus as a function of measured membrane thickness between 293 and 297 K (the range is due to the temperature drop through the samples). The membranes were Nafion® 112, 115, 117 or 1110, all with water content of 22.0 ± 1.0 moles of water per sulphonic acid group, λ . The clamping pressure was 9.3 bar. The contact resistances between the Nafion® membrane and the aluminium surfaces of the apparatus were calculated from the intercept between the regression line and the y-axis and are shown in Table 2.

The thermal resistance and the sample thickness from which the thermal conductivity was calculated, were measured at various humidification levels. All retrieved values are given in Table 2 along with their double standard deviations. λ is the humidification level of Nafion®, denoted as water molecules per sulphonic acid group

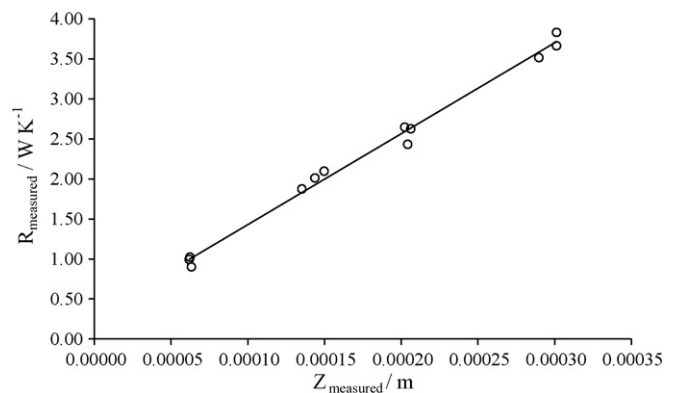


Fig. 5. Measured thermal resistance of Nafion® membranes as a function of the measured membrane thickness. Values include interfacial resistances between Nafion® and the apparatus, found at $295 \pm 2 \text{ K}$, at 22 water molecules per sulphonic group and under 9.3 bar compaction pressure.

in the membrane. The thermal conductivity for Nafion, k_{Nafion} , as a function of water content, λ , at $295 \pm 2 \text{ K}$ is given by Eq. (3.1) and shown in Fig. 6.

$$k_{\text{Nafion}} (\text{W K}^{-1} \text{ m}^{-1}) = (0.177 \pm 0.008) + (3.7 \pm 0.6) 10^{-3} \lambda \quad (3.1)$$

Within the pressure range used (0.5 up to 10 bar) Nafion showed no sign of compressibility, as the externally measured thickness agreed with the thickness measured inside the apparatus within $0\text{--}4 \mu\text{m}$. The measurements at the water level 5 waters per sulphonic group happened to have a large spread without any obvious outliers, thus the large error bars for this point.

Table 1
Measured thickness of Nafion 1110 at various humidification levels, λ .

λ , water per sulphonic group	3	5	11	19	22
$Z_{\text{Nafion}} (\mu\text{m})$	263 ± 3	266 ± 8	271 ± 9	284 ± 12	297 ± 16

Table 2
Thermal properties obtained with Nafion at 295 ± 2 K and over a 3.46 cm^2 large surface at two different compaction pressures.

λ (water level)	4.6 bar		9.3 bar	
	$R''_{\text{Nafion-Al}}$ ($10^{-4} \text{ m}^2 \text{ KW}^{-1}$)	k_{Nafion} ($\text{WK}^{-1} \text{ m}^{-1}$)	$R''_{\text{Nafion-Al}}$ ($10^{-4} \text{ m}^2 \text{ KW}^{-1}$)	k_{Nafion} ($\text{WK}^{-1} \text{ m}^{-1}$)
3.0 ± 1.0	1.41 ± 0.17	0.185 ± 0.007	1.17 ± 0.14	0.187 ± 0.007
5.3 ± 1.0	1.7 ± 0.4	0.19 ± 0.06	1.5 ± 0.3	0.22 ± 0.05
8.7 ± 1.0	1.12 ± 0.08	0.202 ± 0.017	0.89 ± 0.09	0.202 ± 0.015
10.7 ± 1.0	1.1 ± 0.4	0.214 ± 0.015	0.95 ± 0.18	0.219 ± 0.009
14.5 ± 1.0	1.18 ± 0.12	0.228 ± 0.009	1.00 ± 0.07	0.229 ± 0.009
18.9 ± 1.0	1.3 ± 0.2	0.252 ± 0.013	1.08 ± 0.14	0.250 ± 0.010
22.0 ± 1.0	0.7 ± 0.3	0.25 ± 0.02	0.5 ± 0.2	0.254 ± 0.014

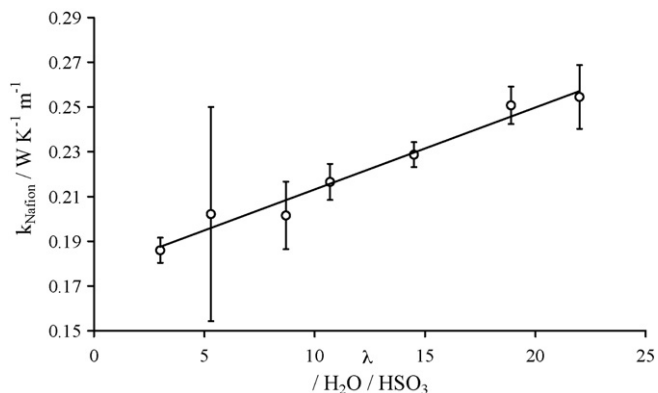


Fig. 6. Thermal conductivity of Nafion membranes at various humidification levels, λ , at 295 ± 2 K. The average is taken between the two series at 4.6 and 9.3 bar compaction pressure.

3.3. Thermal conductivity of the porous transport layer

Fig. 7 presents the measured thermal resistance at various compaction pressures as functions of the measured thickness, both for stacked material and for the single papers. The stacked pieces were put together in a manner so that they would give an average disk thickness outside the apparatus of $270 \pm 2 \mu\text{m}$.

Stacking disks of the same size can only give two true independent equations, one for one disk and a second for multiple amounts of disks, while there are three unknowns, R_{sample} , $R_{\text{sample-sample}}$ and $R_{\text{sample-apparatus}}$. This is due to the linear dependency of unknowns in the stack. Ramousse et al. [8] give estimates based on physical limitations, by saying that the contact resistance to the apparatus must be in the range equal to the thickness of a carbon fibre of air (at the most) or carbon (at the least). Because we have measured the resistance both by stacking (Eq. (2.5)) and changing the thickness (Eq. (2.4)) we have shown that in this case, the thermal

Table 3

Thermal contact resistances retrieved from measurements performed on single PTLs, stacks of PTLs, at various compaction pressures and at 295 ± 2 K.

P (bars)	Eq. (2.4), single	Eq. (2.5), stack
	$2R''_{\text{PTL-Al}}$ ($10^{-4} \text{ m}^2 \text{ KW}^{-1}$)	$2R''_{\text{PTL-Al}} + R''_{\text{PTL-PTL}}$ ($10^{-4} \text{ m}^2 \text{ KW}^{-1}$)
4.6	5 ± 2	4.9 ± 1.5
9.3	3.3 ± 0.9	3.6 ± 1.0
13.9	2.4 ± 0.7	2.8 ± 0.8

resistance between two PTLs is negligible. These results are shown in Table 3.

Fig. 7 superimposes the two different experiments, and shows that y-intercept values are very similar between the two experiments. Additionally, using a Student's t -distribution comparison of the numbers in Table 3, we concluded (95% confidence) that the y-intercept values obtained from the two approaches (Eqs. (2.4) and (2.5)) were not different for any compaction level and that the thermal contact resistance between two PTLs, $R_{\text{PTL-PTL}}$, is negligible in these measurements. Based on this conclusion, we present the thermal conductivities for the PTL based on stacking multiple samples and neglecting the contact resistance between the samples.

The through-plane thermal conductivity of the dry PTL was measured and is presented along with its measured porosity, ε , in Table 4. It is clear that the thermal conductivity increases significantly with increased applied pressure. Next, water was forced through PTL samples to achieve a residual saturation, s , defined as the volume of water in the sample compared to the pore volume. The thermal conductivities of these PTLs are presented in Table 5.

3.4. Thermal resistance of the single PEMFC

The thermal resistivity of a dry ($\lambda = 3 \pm 1$) Nafion® membrane sandwiched between two MPL-coated PTLs, giving a single PEMFC, was measured at 293 K and 4.6 and 9.3 bar compaction pressure over 3.46 cm^2 . The results were 3.7 ± 1.0 and $3.3 \pm 0.5 \text{ m}^2 \text{ KW}^{-1}$ at the two pressures, respectively.

Table 4

Thermal properties for dry PTL as a function of compaction pressure at 295 ± 2 K.

P (bar)	Porosity ε (%)	Eq. (2.4), stack $R''_{\text{PTL-Al}}$ ($10^{-4} \text{ m}^2 \text{ KW}^{-1}$)	Eq. (2.2), stack k_{PTL} ($\text{WK}^{-1} \text{ m}^{-1}$)
4.6	83 ± 2	2.1 ± 0.6	0.27 ± 0.03
9.3	83 ± 2	1.8 ± 0.8	0.36 ± 0.08
13.9	83 ± 2	1.1 ± 0.3	0.40 ± 0.04

Table 5

Thermal properties for humidified PTL as a function of compaction pressure at 295 ± 2 K.

P (bar)	Saturation s (%)	Eq. (2.4), stack $R''_{\text{Humid PTL-Al}}$ ($10^{-4} \text{ m}^2 \text{ KW}^{-1}$)	Eq. (2.4), stack $k_{\text{Humid PTL}}$ ($\text{WK}^{-1} \text{ m}^{-1}$)
4.6	24 ± 3	0.98 ± 0.02	0.45 ± 0.01
9.3	25 ± 3	0.9 ± 0.5	0.54 ± 0.03
13.9	26 ± 3	0.7 ± 0.7	0.57 ± 0.06

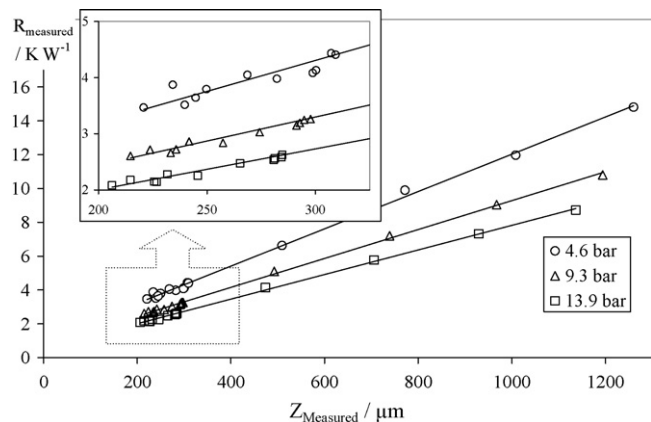


Fig. 7. Measured thermal resistances of single and stacked uncoated PTLs as a function of measured thickness at various compaction pressures and 295 ± 5 K.

Using the thermal resistance of the Nafion® membranes and the PTLs, it is possible to calculate the thermal resistance of the MPL coating plus its membrane–MPL contact. With a thickness of $71 \pm 21 \mu\text{m}$ (measured externally), the thermal conductivity was 0.6 ± 0.6 and $0.5 \pm 0.5 \text{ W K}^{-1} \text{ m}^{-1}$ for the two pressures respectively. The large standard deviation is due to thickness variations.

4. Discussion

Khandelwal and Mench [7] reported a thermal conductivity for Nafion® membrane at the humidification level “it had at arrival from shipping” and at 303 K of $0.16 \pm 0.03 \text{ W K}^{-1} \text{ m}^{-1}$. This is in good agreement with the results of this paper, if we assume that this value refers to the driest value obtainable. This result taken together with the results of the calibration, demonstrate that the apparatus functions well. In addition, the validation reported above demonstrates that the sample to sample resistance can be isolated from the sample to apparatus contact resistance and further the importance of the thickness knowledge.

4.1. Thermal conductivity of Nafion®

The thermal conductivities reported here for the Nafion® membrane as a function of water content are reported, to our knowledge, for the first time. Fig. 6 and Eq. (3.1) reveal that increasing water content, λ , enhances the thermal conductivity of the Nafion® membrane. The increase is more than 40% compared to the level of the driest level. Khandelwal and Mench [7] used volume averaging and the thermal conductivity at the driest level to calculate the thermal conductivity of a fully wetted Nafion membrane. They estimated an increase of approximately 100% compared to the dry membrane [7]. This approach significantly over-predicts the enhancement of the thermal conductivity value. High humidity is crucial for proton conduction through Nafion® membranes and thus the thermal conductivity at high water content is needed in order to predict the correct temperature distribution in an operating PEM fuel cell.

The thermal conductivity of the driest membranes ($\lambda = 3 \pm 1$) was approximately 75% of the thermal conductivity of PTFE. This can be explained by difference in the polymer structure. While Nafion has a branching polymer structure, PTFE has a relatively more streamlined polymer structure. The compaction pressure did not have any effect on the thermal conductivity, however.

The thermal conductivity of Nafion® was found using the assumption that bulk properties of Nafion® do not depend on the membrane thickness. This assumption is reasonable, given the linear relationships in Figs. 5–7.

4.2. Thermal conductivity of the porous transport layer

The assumption to neglect the contact resistance between two PTL samples was shown to be reasonable by comparing results based on Eqs. (2.4) and (2.5). It is clear that scatter between experiments decreases significantly as the applied pressure increases. In this case this is due both to a minimization of the contact resistance between the samples and the apparatus and to an increase in the bulk conductivity of the PTL itself. This increase in bulk conductivity is due to deformation of the fibres and binders in the PTL such that more and better contacts between individual fibres are made with increasing pressure. This presents an interesting challenge for fuel cell modellers as the actual loading (compression) in a fuel cell is not uniform such that a higher conductivity is to be expected under the lands of the bipolar plate as compared to under the channels [9]. In fact, even in the absence of non-homogeneous loading, variations in thickness across a single PTL have a noticeable effect on the thermal conductivity.

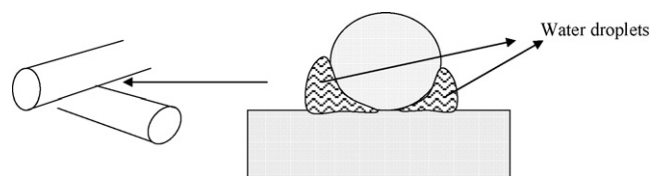


Fig. 8. Sketch of how water droplets may enhance thermal conductivity of a PTL. The figure illustrates two carbon fibres in the PTL.

Comparing Tables 4 and 5 it is clear that the residual water in the PTL has a strong effect on the measured conductivity and on the contact resistance. This effect is more significant than increasing the clamping pressure. The amount of remaining water in the PTL samples after forcing water through them was reproducible and represented about 25% of the pore volume. This water is in all likelihood located at the intersection of individual carbon fibres, as shown in Fig. 8, and as such, has a significant effect on reducing the contact resistance between the fibres. It is very likely that water is in these same locations during fuel cell operation, and as such the effective conductivity of a PTL should include this effect.

4.3. Thermal conductivity of the single PEMFC

From the resistance of the single PEMFC, and relevant dimensions, we were able to obtain an estimate on the thermal conductivity of the MPL coating and the possible contact between MPL and membrane. The thermal conductivity of the MPL of $0.6 \text{ W K}^{-1} \text{ m}^{-1}$ is more than the double of PTFE and Nafion, which both are construction materials for the layer.

5. Conclusion

The thermal conductivity of Nafion membranes was measured *ex situ* at room temperature as a function of water content. The values were found to be linearly dependent on the amount of water molecules per sulphonic acid group in the membrane, λ ;

$$k_{\text{Nafion}} (\text{W K}^{-1} \text{ m}^{-1}) = (0.177 \pm 0.008) + (3.7 \pm 0.6) 10^{-3} \lambda$$

A method for determining the thermal conductivity of deformable materials as a function of compaction pressure has been demonstrated. The thermal conductivity and the thermal contact resistance to an aluminium plate for an uncoated SolviCore PTL (basis for Batch Number # 205-07-1 and 206-07-1) were determined at various compaction pressures. These two properties were also measured for a humidified PTL. For the dry PTL 4.6, 9.3 and 13.9 bar compaction pressure, the thermal conductivity was found to be 0.27, 0.36 and $0.40 \text{ W K}^{-1} \text{ m}^{-1}$ respectively and the thermal contact resistivity to the apparatus was determined to be 2.1, 1.8 and $1.1 \times 10^{-4} \text{ m}^2 \text{ K W}^{-1}$ respectively. It was shown that the thermal contact resistance between two PTLs is negligible compared to the apparatus contact resistivity. The thermal conductivity of a PTL increases by 40–70% due to a residual liquid saturation of 25%.

Acknowledgement

The Norwegian research council is acknowledged for financial support, grant number 164466/S30.

References

- [1] P.J.S. Vie, Characterisation and Optimisation of the Polymer Electrolyte Fuel Cell, Dr. Thesis, NTNU, Norway, 2002.
- [2] P.J.S. Vie, S. Kjelstrup, *Electrochim. Acta* 49 (2004) 1069–1077.
- [3] G. Elert, *The Physics Hypertextbook*, 2006 (hypertextbook.com/physics/thermal/conduction, January).
- [4] S. He, M.M. Mench, S. Tadigadapa, *Sensors Actuators A* (2005).

- [5] E. Birgersson, M. Noponen, M. Vynnycky, J. Electrochem. Soc. 152 (5) (2005) A1021–A1034.
- [6] J. Ihonen, Development of Characterisation Methods for the Components of the Polymer Electrolyte Fuel Cell. Ph.D. Thesis, Dept. of Chemical Engineering and Technology, Applied Electrochemistry, Stockholm, Kungliga Tekniska Högskolan, 2003.
- [7] M. Khandelwal, M.M. Mench, J. Power Sources 161 (2006) 1106–1115.
- [8] J. Ramousse, S. Didierjean, O. Lottin, D. Maillet, Int. J. Thermal Sci. 23 (February) (2007) (Available online).
- [9] E. Sadeghi, M. Bahrami, N. Djilali, J. Power Sources 179 (April (1)) (2008) 200–208.
- [10] Thermophysical Properties Laboratory web-page, Hot Wire Methods for the Thermal Conductivity Measurement, January 2006, <http://www.tpl.ukf.sk/engl.vers/hot.wire.htm>.
- [11] C.L. Choy, K.W. Kwok, W.P. Leung, F.P. Lau, J. Polym. Sci. Part B: Polym. Phys. 32 (8) (1994) 1389–1397.
- [12] M. Spinnler, Int. J. Heat Mass Transfer 47 (2004) 1305–1312.
- [13] Boedeker Plastics, Inc., Texas 77984, USA, web-page; <http://www.boedeker.com> (October 2006).
- [14] T.A. Zawodzinski, M. Neeman, L.O. Sillerud, S. Gottesfeld, J. Phys. Chem. 95 (1991) 6040–6044.
- [15] T.E. Springer, T.A. Zawodzinski, S. Gottesfeld, J. Electrochem. Soc. 138 (1991) 2334–2342.
- [16] K.K. Pushpa, D. Nandan, R.M. Iyer, J. Chem. Soc., Faraday Trans 1 84 (6) (1988) 2047–2056.
- [17] G.E.P. Box, W.G. Hunter, J.S. Hunter, Statistics for Experimenters, John Wiley & Sons Inc., 1978.